

# Spectral Distortions at Super-Kamiokande

S. DEV\*and SANJEEV KUMAR†

Department of Physics, Himachal Pradesh University, Shimla 171005,  
INDIA

## Abstract

One of the characteristic features of the Large Mixing Angle (LMA) MSW solution is the rise in the survival probability of electron neutrinos with the decrease in the neutrino energy. We examine the effect of this rise on the recoil electron spectrum at Super-Kamiokande. It is found that the rise in the LMA MSW survival probability at low energies will lead to a noticeable effect on the recoil electron spectrum at Super-Kamiokande.

## 1 Introduction

Neutrino physics is passing through a phase of spectacular development. Vast amount of solar and atmospheric neutrino data have been accumulated and the neutrino deficits have been established to be the consequence of non-standard neutrino physics. The most recent steps in this direction are the pioneering results from SNO and KamLAND experiments. The SNO experiment provided a model independent proof of solar neutrino oscillations and the terrestrial disappearance of reactor  $\bar{\nu}_e$  observed by KamLAND has provided an independent confirmation of the neutrino oscillation solution of the solar neutrino problem (SNP). This has further boosted our confidence in the oscillation solution of the atmospheric neutrino problem (ANP).

The neutral current (NC) measurements at SNO [1] have, conclusively, established the oscillations of the solar neutrinos and after the evidence for terrestrial antineutrino disappearance in a beam of electronic antineutrinos reported by KamLAND [2], all other solutions [3, 4, 5] of SNP can, at best, be just sub-dominant effects. In fact, KamLAND is the only experiment to explore the neutrino parameter space relevant to SNP with a beam of terrestrial neutrinos

---

\*dev5703@yahoo.com

†sanjeev3kumar@yahoo.co.in

and has convincingly demonstrated the existence of the neutrino oscillations confined to the Large Mixing Angle (LMA) region. The total event rate as well as the distortions in the neutrino spectrum observed at KamLAND are in good agreement with the LMA expectations. However, even after the confirmation of the LMA MSW mechanism as a dominant solution of the SNP, the oscillation parameters are not precisely known. A precise determination of these parameters will be of great importance for theory as well as phenomenology of neutrino oscillations, in particular and particle physics, in general.

The solar neutrino experiments have, already, entered a phase of precision measurements for oscillation parameters. The completeness of the LMA solution is being questioned [6] and the scope for some possible sub-dominant transitions is being explored vigorously [7, 8, 9, 10, 11]. This is because apart from neutrino mass, neutrino flavor oscillations can, also, be generated by a variety of nonstandard neutrino interactions/ properties. In fact, some of these scenarios were invoked earlier as explanations for the SNP alternative to the oscillations. The KamLAND observation of the oscillations of reactor antineutrinos with oscillation parameters in the LMA region has, unambiguously, ruled out these mechanisms as alternative explanations of the SNP. But the existence of these mechanisms at a sub-dominant level is not ruled out by the existing data. The presence of these ‘new physics’ (NP) effects [11] even at a sub-dominant level will affect the present determination of the oscillation parameters. Therefore, LMA solution is facing a deeper scrutiny.

Does the LMA solution, satisfactorily, explain all the solar neutrino data? Are there any observations indicating new physics beyond LMA? These are some of the relevant questions being posed. In fact, some generic predictions of LMA provide enough hints for new physics beyond LMA. It is, therefore, high time to subject the LMA solution to a deeper experimental scrutiny. The direct signatures characterizing the LMA MSW solution are the day-night asymmetry, transition from matter-dominated to vacuum-dominated mixing at low energies and the spectral distortions induced by this transition [11]. The day-night asymmetry, in which many experimental uncertainties cancel out, is one of the cleanest signatures of the LMA MSW transitions but it is too small (2% for the best fit LMA parameters) to be observed in the near future. Such a small value of asymmetry can be confirmed at about  $4\sigma$  C. L. by a detector at least 7 times larger than SK with photo-cathode coverage of at least 40% and an energy threshold of 6MeV in roughly 10 years of running [12]. The second characteristic feature of the LMA MSW solution is the observation of transition from matter dominated to vacuum dominated mixing at low energies which will, only, be possible with the forthcoming low energy solar neutrino experiments. The third characteristic signature of the LMA MSW solution is the rise in the survival probability of the electronic neutrinos with the decrease in neutrino energy. In the present work, we examine quantitatively the effect of the rise in the LMA MSW survival probability of electronic neutrinos at low energies on the recoil electron spectrum at Super-Kamiokande (SK). It is found that the rise in the LMA MSW survival probability at low energies will lead to a noticeable effect on the recoil electron spectrum at Super-Kamiokande.

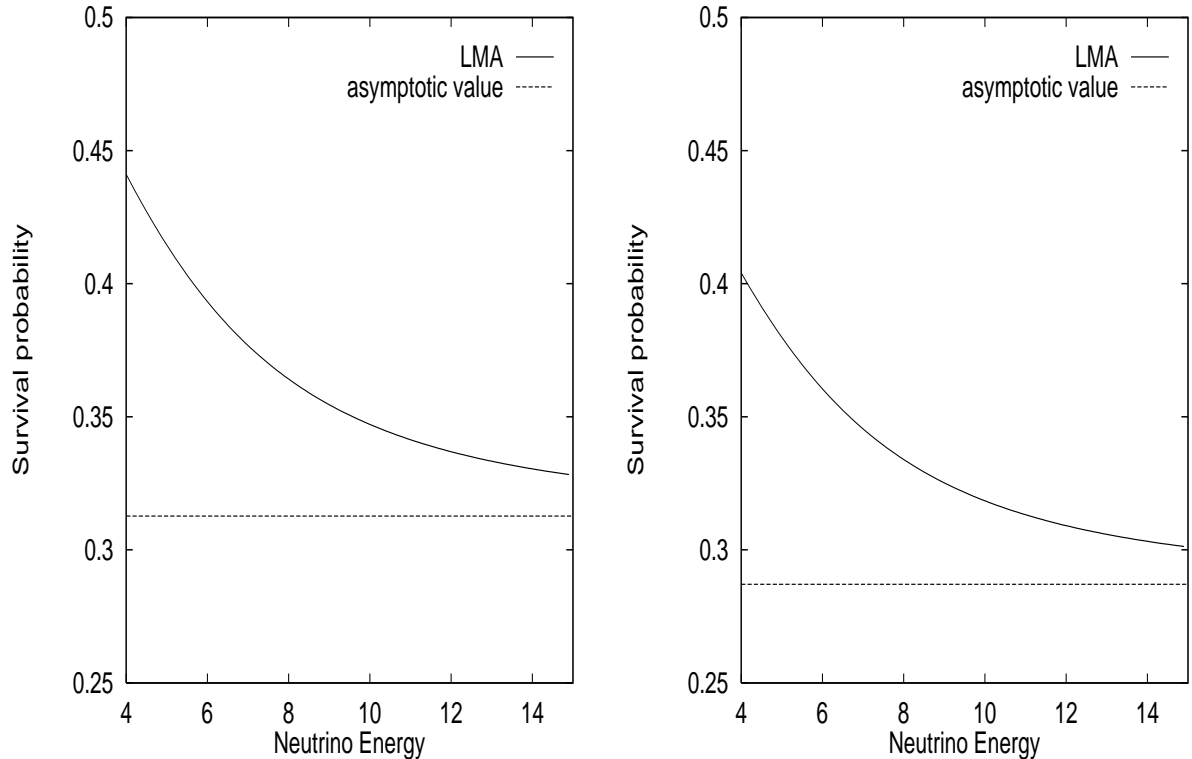


Figure 1: The LMA survival probability for  $\Delta m^2 = 8 \times 10^{-5} eV^2$  and  $\theta_{12} = 34^\circ$  for  $\theta_{13} = 0^\circ$  (left panel) and  $3 \sigma$  CHOOZ bound for  $\theta_{13} = 12.3^\circ$  (right panel).

## 2 LMA MSW survival probability

As of now, the exact profile of the survival probability of electronic neutrinos over the whole energy spectrum remains unknown as a result of which it is not possible to pin point the exact mechanism(s) of neutrino flavor conversion or to exclude the coexistence of the other sub-dominant transitions driven by non-standard neutrino matter-interactions/ properties. The situation is complicated by the fact that the transition probability in some of these non-standard scenarios [13] is energy-independent implying an undistorted solar neutrino spectrum which is consistent with the Super-Kamiokande and SNO spectral data. Consequently, it is extremely important to study the LMA MSW survival probability more carefully since the energy dependence of the mixing angles and eigenstates in matter leads to energy independent survival probability as distinguished from that for simple vacuum mixing. This will result in the distortion of the neutrino energy spectrum in the transition region from matter dominated to vacuum dominated mixing.

In a three flavor scenario, the LMA MSW survival probability for electronic neutrinos to a

very good approximation can be written as [14]

$$P(E) = \cos^4 \theta_{13} \left( \frac{1}{2} + \frac{1}{2} \cos 2\theta_{12} \langle \cos 2\theta_{12}^m \rangle \right) + \sin^4 \theta_{13}, \quad (1)$$

where the mixing angle in matter is given by

$$\cos 2\theta_{12}^m = \frac{\cos 2\theta_{12} - \beta}{\sqrt{(\cos 2\theta_{12} - \beta)^2 + \sin^2 2\theta_{12}}}, \quad (2)$$

and  $\langle \cos 2\theta_{12}^m \rangle$  is obtained by averaging  $\cos 2\theta_{12}^m$  over the production region of the relevant neutrino component [15]. The relative strength of matter dominated to vacuum dominated mixing can be parameterized by a quantity ‘ $\beta$ ’ representing the ratio of matter to vacuum effects:

$$\beta = \frac{\sqrt{2}G_F N_e \cos^4 \theta_{13}}{\Delta m^2 / 2E}. \quad (3)$$

At large energies,  $\beta$  is large and the survival probability approaches the asymptotic matter dominated value given by

$$P_{matter}^{asy} = \cos^4 \theta_{13} \sin^2 \theta_{12} + \sin^4 \theta_{13}. \quad (4)$$

As the energy becomes smaller, the vacuum effects become more important and the survival probability gradually approaches the vacuum value given by

$$P_{vacuum} = \cos^4 \theta_{13} \left( 1 - \frac{1}{2} \sin^2 2\theta_{12} \right) + \sin^4 \theta_{13}. \quad (5)$$

The survival probability has been plotted in Fig. 1 for a typical choice of neutrino parameters in the LMA region viz.  $\Delta m^2 = 8 \times 10^{-5} eV^2$ ,  $\theta_{12} = 34^\circ$  for  $\theta_{13} = 0^\circ$  (left panel) and  $3\sigma$  CHOOZ bound for  $\theta_{13} = 12.3^\circ$  (right panel). The asymptotic value of the matter dominated survival probability has, also, been shown in Fig. 1 for comparison. It is clear that the rise in survival probability at 5MeV from its matter-dominated value is more than 30%. While the survival probability is an increasing function of both  $\Delta m^2$  and  $\theta_{12}$ , the ‘up-turn’ in survival probability is an increasing function of  $\Delta m^2$  and a decreasing function of  $\theta_{12}$  [9]. The ‘up-turn’ in the survival probability of electronic neutrinos at low energies will distort the neutrino energy spectrum and, consequently, the recoil electron spectrum. In the following, we investigate the effect of neutrino spectral distortions at low energies on the recoil electron spectra at SK quantitatively.

### 3 Effect of the ‘up-turn’ on the recoil electron spectra at Super-Kamiokande

The solar boron neutrinos are detected at SK via the following elastic scattering reaction

$$\nu + e \rightarrow \nu + e. \quad (6)$$

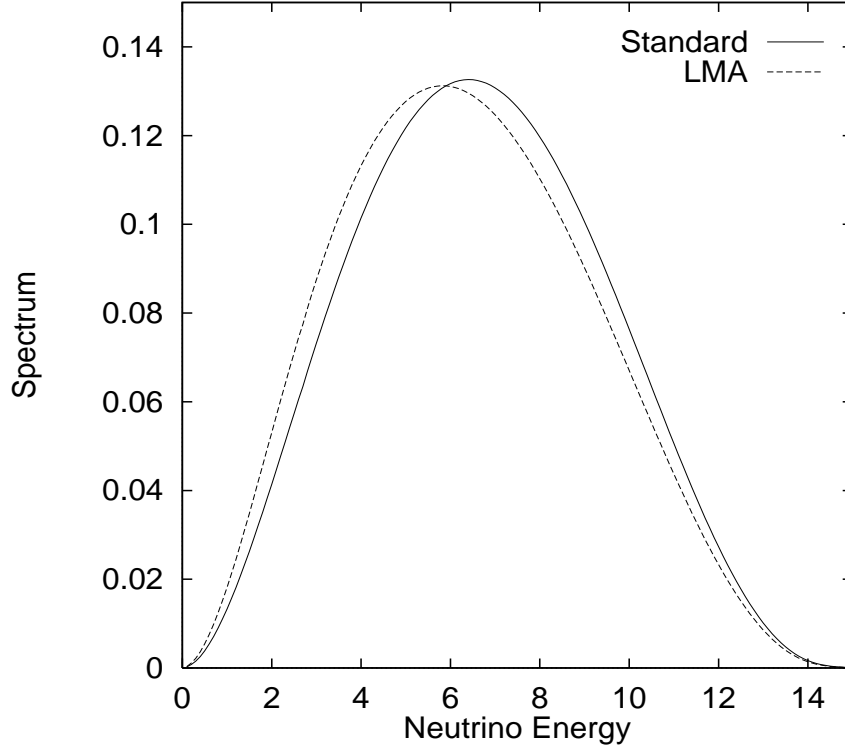


Figure 2: Solar boron neutrino spectrum.

The recoil electron spectrum observed by the detector can be calculated from the spectrum of incoming neutrinos. The standard normalized spectrum for  ${}^8\text{B}$  neutrinos denoted by  $f(E)$  is depicted in Fig. 2. However, this spectrum is modified by the energy dependent LMA MSW survival probability and the modified normalized spectrum is given by

$$f'(E) = \frac{f(E)P(E)}{\int_0^\infty f(E)P(E)dE}. \quad (7)$$

The LMA modified normalized spectrum has, also, been depicted in Fig. 2 along with the standard normalized spectrum for comparison. Clearly, the energy dependence of the LMA MSW survival probability leads to substantial changes in the emergent neutrino spectrum. In the following, we quantitatively investigate the effect of the standard undistorted  ${}^8\text{B}$  neutrino spectrum and the LMA distorted boron neutrino spectrum on the recoil electron spectrum at Super-Kamiokande.

The averaged differential cross-section for the production of a recoil electron with the kinetic energy  $T$  by incoming neutrinos with the spectrum  $f(E)$  is given by

$$\left\langle \frac{d\sigma}{dT} \right\rangle = \int_{E_{\min}}^{E_{\max}} dE f(E) \left[ \frac{d\sigma_e}{dT} P(E) + \frac{d\sigma_x}{dT} \{1 - P(E)\} \right] \quad (8)$$

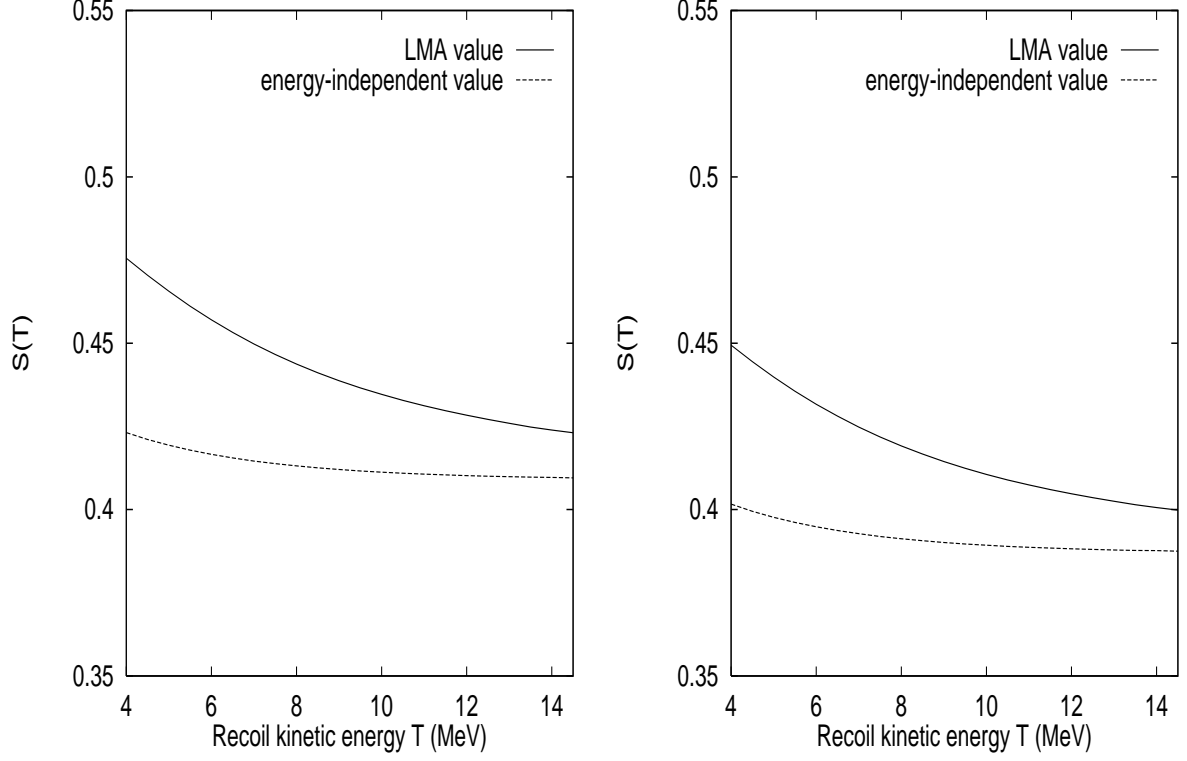


Figure 3:  $S(T)$  versus  $T$  for  $\theta_{13} = 0^\circ$  (left panel) and  $\theta_{13} = 12.3^\circ$  (right panel).

where the cross-sections for  $\nu_e e$  and  $\nu_x e$  ( $x = \mu, \tau$ ) scattering are given by

$$\frac{d\sigma_e}{dT} = \frac{2G_F^2 m_e^2}{\pi^4} \left[ g_{eL}^2 + g_R^2 \left( 1 - \frac{T}{E} \right)^2 - g_{eL} g_R \frac{m_e T}{E^2} \right] \quad (9)$$

and

$$\frac{d\sigma_x}{dT} = \frac{2G_F^2 m_e^2}{\pi^4} \left[ g_{xL}^2 + g_R^2 \left( 1 - \frac{T}{E} \right)^2 - g_{xL} g_R \frac{m_e T}{E^2} \right] \quad (10)$$

respectively with  $g_R = \sin^2 \theta_W$ ,  $g_{eL} = \frac{1}{2} + \sin^2 \theta_W$  and  $g_{xL} = -\frac{1}{2} + \sin^2 \theta_W$  [16]. The minimum energy  $E_{\min}$  is fixed by the kinematics to be

$$E_{\min} = \frac{T + \sqrt{T(T + 2m_e T)}}{2} \quad (11)$$

and  $E_{\max}$  is the neutrino end point energy. In order to study the effect of the rise in the electron survival probability on the recoil electron spectrum, we define a quantity  $S(T)$  as

$$S(T) = \frac{\left\langle \frac{d\sigma}{dT} \right\rangle_{LMA}}{\left\langle \frac{d\sigma}{dT} \right\rangle_{SSM}}, \quad (12)$$

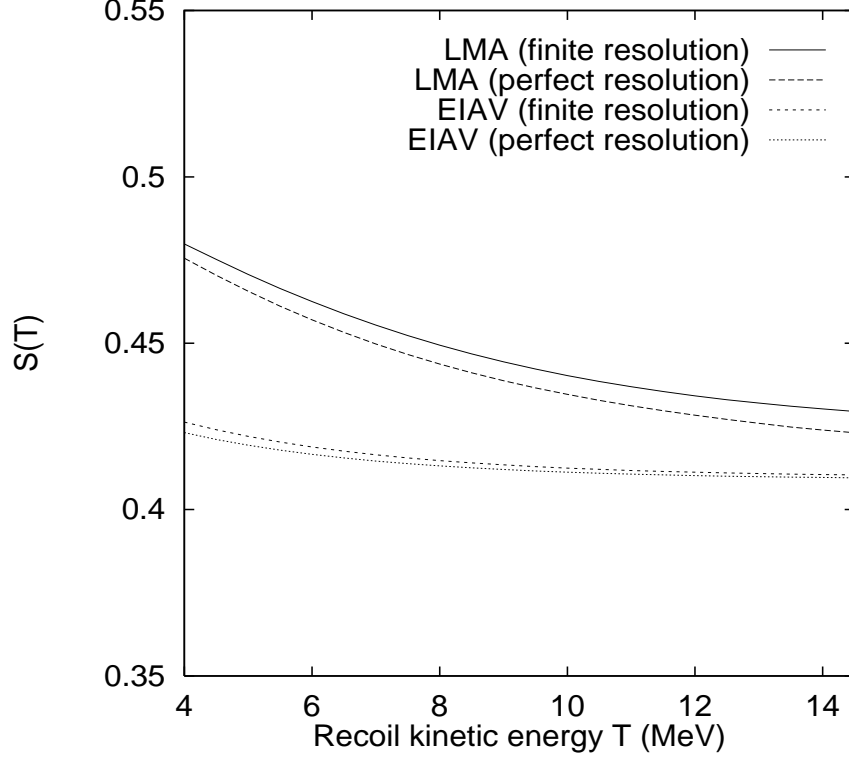


Figure 4: Probability folded with detector response function and neutrino cross-sections as the function of recoil electron kinetic energy.

$$= \frac{\int_{E_{\min}}^{E_{\max}} dE f(E) \left[ \frac{d\sigma_e}{dT} P(E) + \frac{d\sigma_x}{dT} \{1 - P(E)\} \right]}{\int_{E_{\min}}^{E_{\max}} dE f(E) \frac{d\sigma_e}{dT}}, \quad (13)$$

which has the interpretation as the probability of an electron being scattered with a recoil kinetic energy  $T$  and closely resembles the SK data/SSM ratio with the only difference that the SK data/SSM ratio is presented for individual energy bins while  $S(T)$  as defined above is a continuous function of recoil electron energy. In fact,  $S(T)$  is the LMA expectation for the recoil electron spectrum normalized to the standard  $^8\text{B}$  neutrino spectrum and has been plotted as a function of  $T$  in Fig. 3 along with the  $S(T)$  for energy-independent asymptotic value of the LMA survival probability for comparison. The two probabilities differ considerably from each other and this difference could be as large as 10% at 5 MeV. This is enough to highlight the role of spectral distortions in discriminating the LMA suppression scenario from the energy independent suppression NP scenarios mentioned above. At the current level of precision, both the LMA suppression and the energy-independent suppression are consistent with the SK as well as SNO solar neutrino data. Consequently, one can not claim a conclusive confirmation of the LMA solution from the exclusive study of the high energy region of the solar neutrino spectrum. It is, therefore, imperative to study quantitatively the spectral distortions not only to finally confirm the LMA solution but

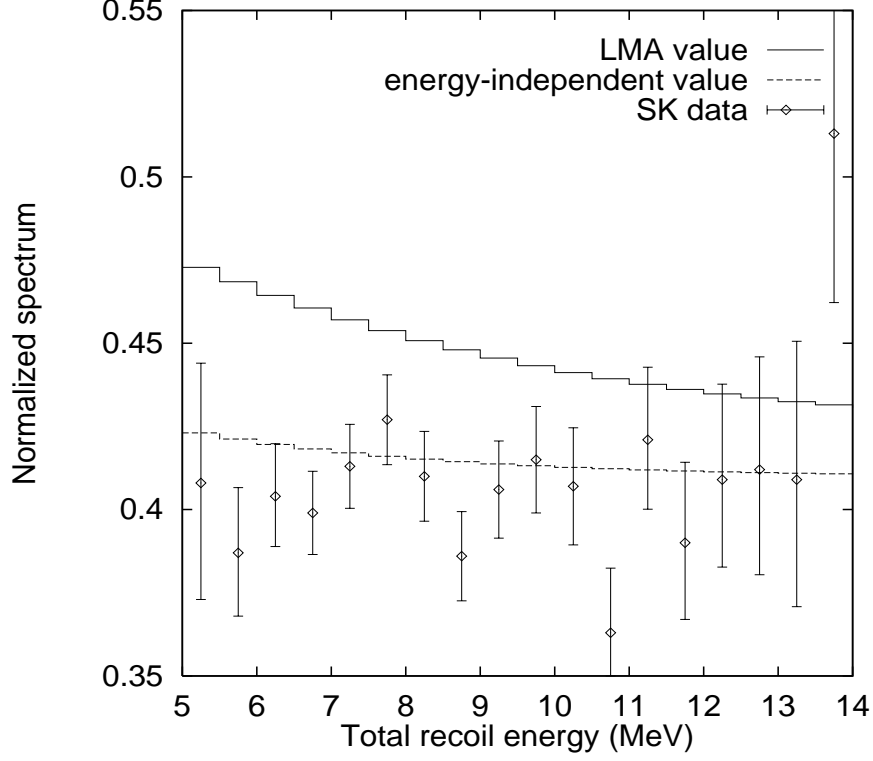


Figure 5: The recoil electron spectrum normalized to SSM in the bins of 0.5 MeV ( $\mathcal{S}$ ). The SK data with statistical errors is also shown for comparison.

also to disentangle the possible NP effects. So, we embark upon a quantitative study of spectral distortions at SK because of its better precision by taking into account the finite energy resolution of SK to see whether the LMA spectrum can be differentiated from an undistorted spectrum at SK.

The measured energy of a recoil electron, in general, is normally distributed around the actual energy with a spread that depends on the actual energy of the recoil electron. The probability that a recoil electron with true kinetic energy  $T_{true}$  will be detected with the observed kinetic energy  $T_{obs}$  is given by

$$r(T_{true}, T_{obs}) = \frac{1}{\sqrt{2\pi}\sigma_T} \exp\left(-\frac{(T_{true} - T_{obs})^2}{2\sigma_T^2}\right) \quad (14)$$

and is called the detector response function. The energy-dependent spread,  $\sigma_T$ , is of the form

$$\sigma_T = \epsilon \sqrt{\frac{T_{true}}{10 \text{ MeV}}} \quad (15)$$

so that  $\epsilon$  is the energy spread at 10 MeV. For SK,  $\epsilon = 1.4$ . To account for the finite energy resolution, the differential cross-section must be folded with the detector response function,



i.e. we must have

$$\left\langle \frac{d\sigma}{dT} \right\rangle (T_{obs}) = \int_0^\infty dT_{true} \left\langle \frac{d\sigma}{dT} \right\rangle (T_{true}) r(T_{true}, T_{obs}) \quad (16)$$

in Eq. (13) for  $S(T)$  to obtain the observed value of

$$S(T_{obs}) = \frac{\int_0^\infty dT_{true} r(T_{true}, T_{obs}) \int_{E_{min}}^{E_{max}} dE f(E) \left[ \frac{d\sigma_e}{dT_{true}} P(E) + \frac{d\sigma_x}{dT_{true}} \{1 - P(E)\} \right]}{\int_0^\infty dT_{true} r(T_{true}, T_{obs}) \int_{E_{min}}^{E_{max}} dE f(E) \frac{d\sigma_e}{dT_{true}}}. \quad (17)$$

Note that the integration over  $T_{true}$  is meaningful only in a small interval around  $T_{obs}$  because the detector response function  $r(T_{true}, T_{obs})$  falls rapidly as we go away from  $T_{obs}$  in either direction. The quantity  $S(T_{obs})$  has been plotted as a function of  $T_{obs}$  in Fig. 4 for the LMA value of survival probability as well as the energy independent asymptotic value (EIAV) of the survival probability. Also shown are the same two curves depicted in Fig. 3 assuming perfect energy resolution. It is clear that the finite energy resolution has resulted in a slight increase in the value of  $S(T_{obs})$  for the LMA solution and this increase is more pronounced at the larger energies. However,  $S(T_{obs})$  changes very little for the energy-independent asymptotic value of the survival probability. The quantity  $S(T_{obs})$  has to be integrated over the recoil kinetic energy  $T_{obs}$  in order to make it an observable quantity. We integrate  $S(T_{obs})$  over the total recoil electron energy  $E_{obs} = T_{obs} + m_e$  in the bins of 0.5 MeV. This integrated normalized spectrum is denoted by  $\mathcal{S}$  and has been plotted in Fig. 5 alongwith the actual 1496 day SK spectrum normalized to BP04 with statistical errors only [17].

One can calculate the rise in the LMA value  $S_{LMA}(T_{obs})$  relative to the energy independent asymptotic value  $S_{EIAV}(T_{obs})$  at a particular value of  $T_{obs}$  by defining

$$R(T_{obs}) = \frac{S_{LMA}(T_{obs}) - S_{EIAV}(T_{obs})}{S_{EIAV}(T_{obs})}. \quad (18)$$

It is instructive to see the variation in  $R(T_{obs})$  because of the energy spread  $\epsilon$ . Fig. 6 shows  $R(T_{obs})$  for  $\epsilon = 0$  (perfect energy resolution) and for  $\epsilon = 1.4$  (finite energy resolution). It is clear that as a result of finite energy resolution of the detector,  $S_{LMA}(T_{obs})$  and, therefore,  $R(T_{obs})$  gets enhanced as compared to the corresponding values for perfect energy resolution and, again, this increase is more pronounced at the higher energies. Although, the curve for  $R(T_{obs})$  becomes flatter because of the finite energy resolution of the detector, but the actual value of  $R(T_{obs})$  becomes larger which is an advantage. Therefore, one possible way to look for the spectral distortions is to measure the data/SSM ratio accurately over small energy bins and, then, compare these with the values calculated by assuming the energy-independent asymptotic value of survival probability. Alternatively, one can compare the value of  $\mathcal{S}$  in a low energy bin viz.  $\mathcal{S}_L$  with that in a high energy bin viz.  $\mathcal{S}_H$  and find the relative increase in  $\mathcal{S}$  by defining the relative rise-up  $\mathcal{R}$  as

$$\mathcal{R} = \frac{\mathcal{S}_L - \mathcal{S}_H}{\mathcal{S}_H}. \quad (19)$$

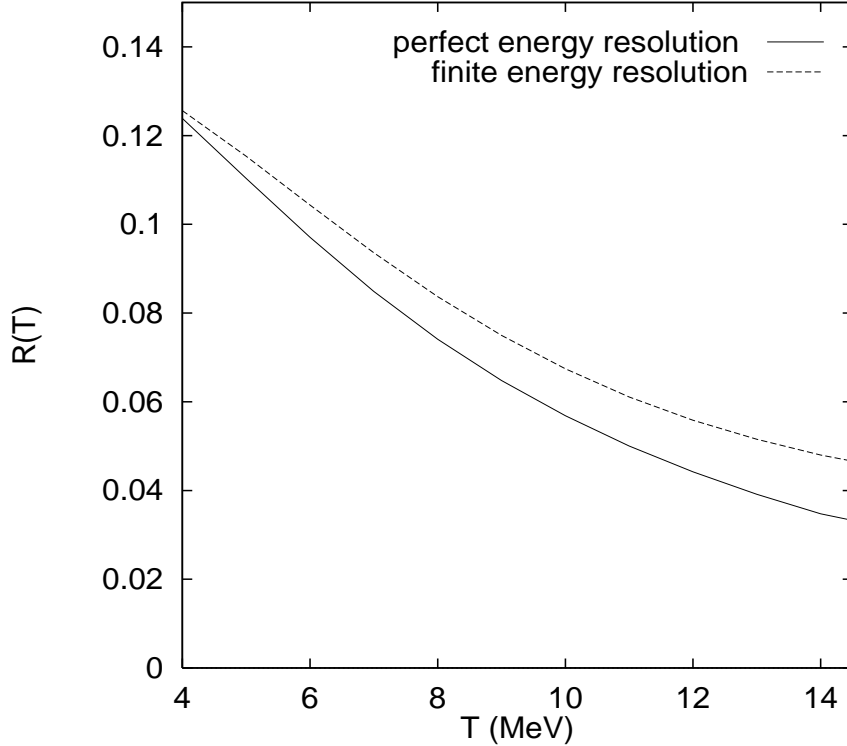


Figure 6:  $R(E_{obs})$  versus  $E_{obs}$ .

It is important to note that  $\mathcal{R}$  defined above is essentially independent of the flux normalization. Otherwise, it would have been difficult to directly compare  $\mathcal{S}$  with the experimental data which has to be normalized to the SSM  $^8B$  flux which is not known accurately enough. Also, the above definition is, almost, independent of  $\theta_{13}$  since the factor of  $\cos^4 \theta_{13}$  cancels in the ratio. A non-zero  $\theta_{13}$  will suppress  $S(T)$  by the factor of  $\cos^4 \theta_{13}$  but the ‘rise-up’  $\mathcal{R}$  will remain practically unchanged (see Fig. 3). Thus, if the SK spectrum is found to differ from the LMA spectrum, this conflict cannot be reconciled even in a 3-flavor framework since the LMA value of  $\mathcal{R}$  is the same in two/three-flavor framework for small  $\theta_{13}$ . This is contrary to some assertions made recently [18] in literature. Moreover, most of the energy correlated systematic uncertainties will cancel in  $\mathcal{R}$ .

The variable  $\mathcal{R}$  defined in Eq. (19) can be used as an observable to quantify the turn-up in the data/SSM ratio at SK at low energies. It is different from the global observables like the moments defined in Ref. [19] in the sense that it directly compares the normalized spectral data at two energy ends of the spectrum while the moments are global quantities which are not suitable for this purpose. Moreover, the SK solar neutrino data is, already, available in small energy bins. For the sake of illustration, we choose the bins  $E = 5.5 - 6.0 MeV$  and

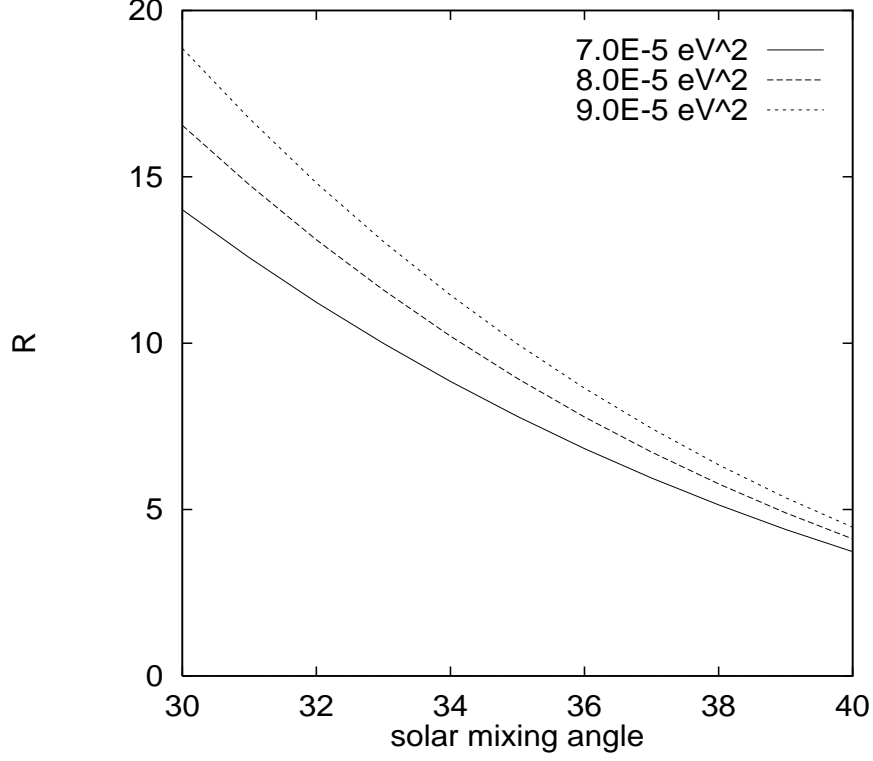


Figure 7:  $\mathcal{R}$  versus  $\theta_{12}$  for different values of  $\Delta m^2$ .

$E = 13.5 - 14.0 \text{ MeV}$  and evaluate  $\mathcal{R}$  for these bins to obtain

$$\mathcal{R} = -0.05 \pm 0.11. \quad (20)$$

Therefore, the rise-up is not significantly different from zero for these energy bins. The upper bound on  $\mathcal{R}$  is approximately 0.06 (0.17) at  $1\sigma$  ( $2\sigma$ ) C.L.. This is to be compared with the corresponding LMA value of rise-up

$$\mathcal{R}_{LMA} = 0.09^{+0.03}_{-0.02} \quad (21)$$

for  $\Delta m^2 = 7.9 \pm 0.3 \times 10^{-5} \text{ eV}^2$  and  $\sin^2 \theta_{12} = 0.3^{+0.02}_{-0.03}$ . This LMA value becomes compatible with the present experimental value [Eq. (20)] at more than  $1\sigma$  C.L..

Now, we examine the prospects for the measurement of a rise-up within the LMA solution. A careful examination of the binned SK-I data [17] reveals that the errors at the high energy end of the recoil electron spectrum are large as compared to the errors at the low energy end. In fact, the ratio of relative errors in  $\mathcal{S}_H$  ( $E=13.5-14.0 \text{ MeV}$ ) to the relative error in  $\mathcal{S}_L$  ( $E=5.5-6.0 \text{ MeV}$ ) is about 2.2 at present. In Fig. 8, we present the required values of the relative errors in  $\mathcal{S}_L$  for the measurement of a rise-up of 9% (LMA value) at different confidence levels for this case. It is clear from Fig. 8 that the statistical errors in  $\mathcal{S}_L$  will

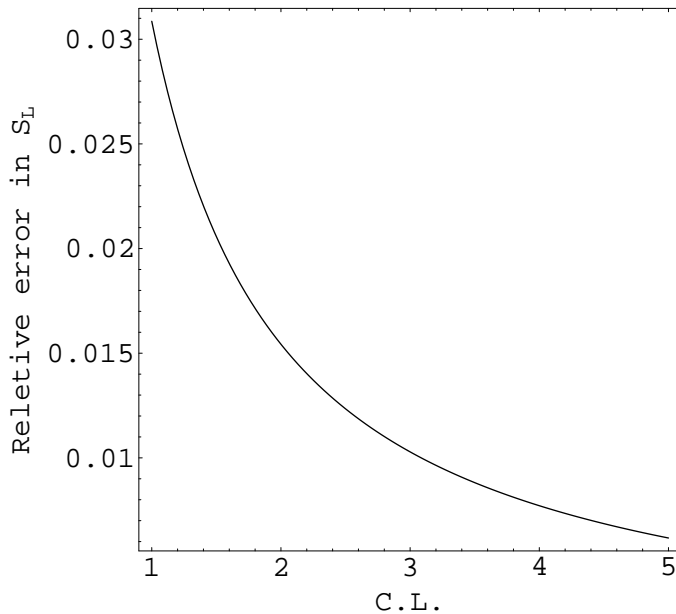


Figure 8: Relative error in  $\mathcal{S}_L$  required for the observation of  $\mathcal{R} = 0.09$  at various confidence levels at SK with the present error ratio (2.7) at high and low energy ends.

have to be reduced below 1% to measure a rise-up of 9% at  $3\sigma$  C.L., for example. However, if the relative errors in the data/SSM ratio at the high energy end are reduced to the same level as the relative errors at the low energy end, considerable improvement results. To see this improvement, we plot the required values of relative errors in  $\mathcal{S}_L$  as a function of  $\mathcal{R}$  at  $1\sigma$ ,  $2\sigma$  and  $3\sigma$  confidence levels in Fig. 9a for this case. It can be seen that with equal statistical errors in  $\mathcal{S}$  at high and low energy ends of the recoil electron spectrum and if the statistical errors are reduced by half, a rise-up as large as 8% (13%) can be measured at  $2\sigma$  ( $3\sigma$ ) C.L. at SK. In Fig. 9b, the requisite values of relative errors in  $\mathcal{S}_L$  for the measurement of a rise-up  $\mathcal{R} = 0.09$  at  $1\sigma$ ,  $2\sigma$  and  $3\sigma$  confidence levels have been plotted as a function of the ratio of relative errors at the high and low energy ends of the neutrino spectrum. It is clear from Fig. 9b that this ratio must be reduced below 0.6 in order to measure a rise-up of 9% at more than  $3\sigma$  C.L. with the statistical errors in  $\mathcal{S}_L$  reduced to less than half of the present value. However, the present analysis is only illustrative since the systematic errors have not been incorporated in the analysis. A more elaborate analysis is in progress and will be presented elsewhere.

The ‘rise-up’  $\mathcal{R}$  has been plotted in Fig. 7 as a function of  $\theta_{12}$  for different values of  $\Delta m_{12}^2$ . The rise-up in data/SSM ratio is large enough to be noticeable in the SK recoil electron spectrum. Since, the rise-up  $\mathcal{R}$  becomes larger for smaller values of  $\theta_{12}$ , an upper bound on  $\mathcal{R}$  can be used to obtain a lower bound on  $\theta_{12}$  [9].

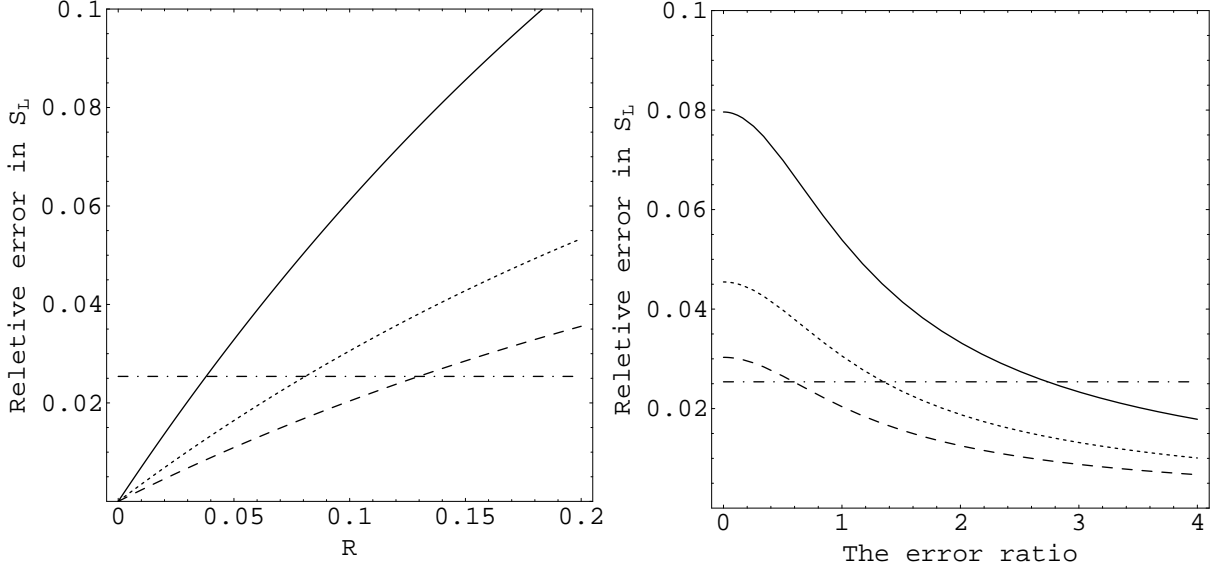


Figure 9: (a) Relative errors in  $\mathcal{S}_L$  as a function of  $\mathcal{R}$  for equal errors in  $\mathcal{S}_L$  and  $\mathcal{S}_H$  (left panel). (b) Relative errors in  $\mathcal{S}_L$  as a function of the ratio of the relative errors in  $\mathcal{S}_H$  and  $\mathcal{S}_L$  for  $\mathcal{R} = 0.09$  (right panel). The horizontal line represents half of the present statistical error. The solid, dotted and dashed lines are at 1, 2 and 3  $\sigma$  respectively.

The enhancement in  $S(T)$  for smaller values of  $T$  can be used to further constrain the currently allowed neutrino parameter space. We illustrate this point by plotting the constant  $\mathcal{S}$  and  $\mathcal{R}$  curves on the  $(\Delta m_{12}^2, \theta_{12})$  plane. The quantity  $\mathcal{S}$  is obtained by integrating  $S(T)$  over the energy bin of 0.5 MeV centered around  $T=5$  MeV and the quantity  $\mathcal{R}$  is calculated from Eq. (19) for the energy bins of 0.5 MeV centered around  $T=5$  MeV, 15 MeV. We choose these values for illustrative purposes only. The constant  $\mathcal{S}$  and  $\mathcal{R}$  curves on the  $(\Delta m_{12}^2, \theta_{12})$  plane are shown in Fig. 7 for the  $(\Delta m_{12}^2, \theta_{12})$  parameter space within the currently allowed LMA region. For  $\Delta m_{12}^2$  and  $\theta_{12}$ , we select the  $2\sigma$  ranges of these quantities and plot the constant  $\mathcal{S}$  curves for  $\mathcal{S} = 0.44, 0.46, 0.48$  (curves with negative slope from left to right, respectively) and, also, plot the constant  $\mathcal{R}$  curves for  $\mathcal{R} = 0.12, 0.10, 0.8$  (curves with positive slope from left to right, respectively). It is evident that there is an increase in  $\mathcal{S}$  and decrease in  $\mathcal{R}$  with increasing  $\theta_{12}$ . Therefore, an accurate measurement of  $\mathcal{S}$  and  $\mathcal{R}$  at 5MeV will further constrain the LMA allowed  $\theta_{12}$ . For instance, if  $\mathcal{S}$  is found to be greater than 0.44 (i.e.  $\mathcal{S} \geq 0.44$ ) and  $\mathcal{R}$  is found to be less than 10% (i.e.  $\mathcal{R} \leq 10\%$ ),  $\theta_{12}$  will, approximately, be within the range  $32^\circ \leq \theta_{12} \leq 34^\circ$ .

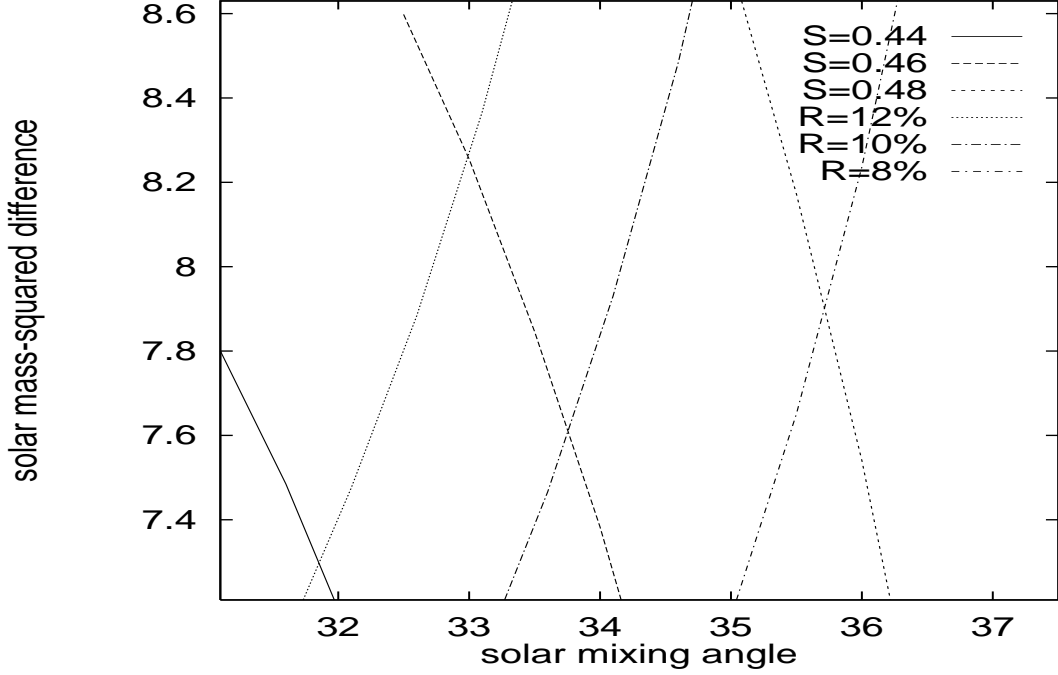


Figure 10: Constant  $\mathcal{S}$  and  $\mathcal{R}$  plots.

## 4 Conclusions

Out of the direct signatures characterizing the LMA MSW solution viz. the day-night asymmetry, vacuum-dominated mixing at low energies and the distortions in the recoil electron spectra because of the rise in the LMA MSW survival probability at low energies, only the last signature has a good chance of being observed in the immediate future at SK because of its better precision. Accordingly, we examined the effect of the rise in the LMA MSW survival probability on the recoil electron spectrum at SK. It is found that the quantity  $S(T)$  increases by about 10% in going from 15 MeV to 5 MeV and is large enough to be noticeable at SK especially after the SK collaboration lowers the detection threshold and reduces the systematic and statistical errors, especially at the high energy end which serves as a reference point for the measurement of rise-up. Thus, the prospects for the observation of spectral distortions at SK-III, in case it comes up, appear to be bright [19]. The failure to observe spectral distortions at SK-III would signal new physics beyond LMA. If the SK spectrum is found to be different from the LMA spectrum, this conflict cannot be reconciled even in a three flavor framework with a non-zero  $\theta_{13}$ . The rise in  $S(T)$  depends on  $\theta_{12}$  and this rise becomes larger for smaller values of  $\theta_{12}$ . Accordingly, a measurement of the spectral up-turn can be used to further constrain the currently allowed LMA parameter space.

## 5 Acknowledgments

We thank the learned referee of Phys. Rev. D for the constructive criticism which resulted in considerable improvements in the manuscript. The research work of S. D. is supported by the Board of Research in Nuclear Sciences (BRNS), Department of Atomic Energy, Government of India *vide* Grant No. 2004/ 37/ 23/ BRNS/ 399. S. K. acknowledges the financial support provided by Council for Scientific and Industrial Research (CSIR), Government of India.

## References

- [1] B. Aharmin *et al* (SNO Collab.), nucl-ex/0502021.
- [2] K. Eguchi *et al* (KamLAND Collab.), *Phys. Rev. Lett.* **90**, 021802 (2003).
- [3] C. S. Lim and W. J. Marciano, *Phys. Rev.* **D37**, 1368 (1988).
- [4] B. C. Chauhan, S. Dev and U. C. Pandey, *Phys. Rev.* **D59**, 083002 (1999).
- [5] E. Kh. Akhmedov and J. Pulido, *Phys. Lett.* **B 485**, 178 (2000), *ibid.*, **B 553**, 7 (2003).
- [6] A. Yu. Smirnov, arXiv:hep-ph/0305106 v2.
- [7] P. C. de Hollanda and A. Yu. Smirnov, *Phys. Rev.* **D69**, 113002 (2004).
- [8] Bhag C. Chauhan and João Pulido, arXiv:hep-ph/0402194.
- [9] S. Dev and Sanjeev Kumar, *Mod. Phy. Lett.* **20**, 2083, (2005).
- [10] S. Dev and Sanjeev Kumar, *Mod. Phy. Lett.* **20**, 2957, (2005).
- [11] H. Back *et el*, arXiv:hep-ex/0412016 and references therein.
- [12] J. N. Bahcall and C. Pena-Garay, *JHEP* **0311**, 004 (2003).
- [13] J. W. F. Valle, *Prog. Part. Nucl. Phys.* **26**, 91, (1991); *Phys. Lett.* **B 199**, 432, (1987).
- [14] S. J. Parke, *Phys. Rev. Lett.* **57**, 1275, (1986).
- [15] J. N. Bahcall, *Nuc. Phys. (Proc. Suppl.)*, **B118**, 77 (2003).
- [16] G. t'Hooft, *Phys. Lett.* **B37**, 195, (1971).
- [17] J. Hosaka *et al*, (Super-Kamiokande Collab.), hep-ex/0508053.
- [18] Bipin Singh Koranga, Mohan Narayan, and S. Uma Sankar, arXiv:hep-ph/0503029.
- [19] J. N. Bahcall, P. I. Krastev and E. Lisi, *Phys. Rev.* **C 55**, 494, (1997).
- [20] K. Ishihara [Super-Kamiokande Collab.], Invited Talk at ICHEP04 (2004).